Biodistribution of a Positron-Emitting Suicide Inactivator of Monoamine Oxidase, Carbon-11 Pargyline, in Mice and a Rabbit

Kiichi Ishiwata, Tatsuo Ido, Kazuhiko Yanai, Koichiro Kawashima, Yuka Miura, Minoru Monma, Shoichi Watanuki, Toshihiro Takahashi, and Ren Iwata

Division of Radioisotope Research, Cyclotron and Radioisotope Center, Tohoku University, Sendai, 980, Japan.

Carbon-11 (^{11}C) pargyline, which is a suicide inactivator of Type B monoamine oxidase (MAO), was synthesized by the reaction of *N*-demethylpargyline with $^{11}CH_3I$. Biodistribution was investigated in mice, and positron tomographic images of the heart and lung in a rabbit were obtained. The distribution of ^{11}C after administration of [^{11}C]pargyline was measured in several organs and blood at various time intervals. After 30 min its concentrations in the organs were constant. Subcellular distribution studies in the brain, lung, liver, and kidney showed that 59–70% of the ^{11}C became acid-insoluble and 9–33% was present in the crude mitochondrial fraction at 60 min after injection. However, a high loading dose influenced the subcellular distribution but had little effect on tissue distribution. The uptakes of the ^{11}C in each organ except for the kidney and spleen seemed to correlate with the in vitro enzymatic activity of Type B MAO. At high loading dose a nonspecific uptake was observed.

J Nucl Med 26:630–636, 1985

Positron emission tomography (PET) can evaluate some in vivo metabolism, such as glucose consumption, oxygen utilization, and protein synthesis (*1*). Direct evaluation of enzyme activities or enzyme concentration is an interesting objective for PET study, especially in studies of diseases with aberrant metabolism. This objective will require the development of new radiopharmaceuticals. Suicide inactivators of enzymes, which are interesting enzymatically and pharmacologically, are of interest because they bind irreversibly to target enzymes (*2*). Several propynylamines are suicide inactivators of the monoamine oxidase (MAO) (*3–6*), and the hydrogen-3 or carbon-14- (^{14}C) labeled compounds have been synthesized for enzyme studies (*7,8*). Monoamine oxidase is widely distributed in many organs, plays important roles in amine metabolism, and two enzyme species, Type A and Type B, are present depending on their substrate specificity. We describe here the synthesis of *N*-benzyl-*N*-[^{11}C]methyl 2-propynylamine([^{11}C]-pargyline), a specific inhibitor for the Type B MAO, by the reaction of *N*-demethylpargyline with $^{11}CH_3I$ and its biodistribution in mice and a rabbit, and discuss the problems of using a suicide inactivator for evaluating enzyme activity.

Received Oct. 1, 1984; revision accepted Feb. 11, 1985.

For reprints contact: Kiichi Ishiwata, PhD, Div. of Radioisotope Research, Cyclotron and Radioisotope Center, Tohoku University, Aoba, Aramaki, Sendai, 980, Japan.

MATERIALS AND METHODS

Synthesis of [^{11}C]pargyline (Scheme I)

[^{11}C]CH_3I was prepared from $^{11}CO_2$ by reduction with $LiAlH_4$ and distillation of [^{11}C]methanol in a helium stream through refluxing HI by using an automated synthesis system (*9,10*). $^{11}CH_3I$ was trapped in 1.5 ml acetone containing 5–10 mg *N*-benzyl 2-propynylamine* (without further purification) at dry-ice acetone temperature. The solution was heated at 50–60°C for 5–10 min. Unreacted $^{11}CH_3I$ was swept with a helium stream of 200 ml/min for 2–3 min at 50–60°C. Acetone was also removed with a helium stream. The residue was dissolved in 300 μl of 60% MeOH and subjected to high

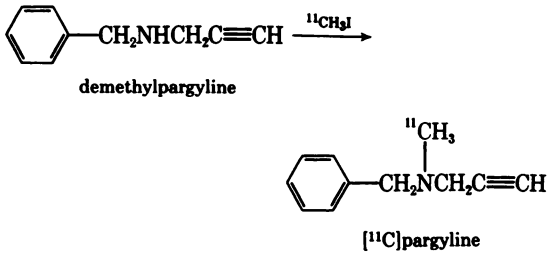

Scheme I

performance liquid chromatography (HPLC), using uv and radioactivity monitors (radio-HPLC) on a μBondapak C18 column.† Elution was performed with a MeOH-H_2O (60/40, v/v) mixture at a flow rate of 2 ml/min. The [^{11}C]pargyline fraction was collected, acidified with four drops of 0.1*M* HCl and evaporated to dryness. The [^{11}C]pargyline was dissolved in saline, neutralized with 0.1*M* NaOH and filtered through a membrane filter (0.22 μm). Radiochemical purity was analyzed by the above chromatographic system. The [^{11}C]pargyline was thus obtained for animal experiments with a radiochemical yield of 22–45% and a radiochemical purity of over 99% in a time of 50–60 min. The specific activity was determined to be 10–40 Ci/mmol at the time of use by uv-response on the same HPLC system described above using authentic pargyline.‡

Biodistribution in mice

GDY mice were injected i.v. with no-carrier-added [^{11}C]pargyline (0.2 mCi/0.2 ml, 30–130 μg/kg). At various times, mice were killed by cervical dislocation, and tissues were removed and washed with saline. The tissues were weighed and the radioactivity was measured with a gamma-ray detector.§ The uptake was expressed as the differential absorption ratio (DAR), (count/g tissue) × (g body weight/total injected count).

TABLE 1
Synthesis of [^{11}C]Pargyline

Run no.	Reaction conditions: *N*-desmethyl-pargyline (mg)	Temperature (°C)	Time (min)	Overall yield of [^{11}C] pargyline (%)
1	9.9	65	10	30.2
2	9.3	60	10	44.6
3	9.7	57	10	22.0
4	4.9	60	10	32.0
5	5.5	50	10	32.8
6	5.1	60	5	31.8
7	5.1	53	5	24.1

Effect of loading dose

Pargyline hydrochloride was obtained commercially.‡ Mice were injected with loading doses of 0.5–63 mg/kg, and the distribution was measured at 30 min after injection of [^{11}C]pargyline.

Subcellular distribution

0.2–0.5 g of the brain, lung, kidney, or liver was homogenized in 3 ml of 0.3*M* sucrose with a Teflon-glass homogenizer. The homogenate was centrifuged at 1,500 rpm for 10 min. The pellet was suspended in 3 ml of 0.3*M* sucrose and centrifuged again. The pellet was the nuclear fraction. The combined supernatant was centrifuged at 10,000 rpm for 10 min. The pellet was suspended in 3 ml of 0.3*M* sucrose and centrifuged. This pellet was the crude mitochondrial fraction and the supernatant was the postmitochondrial fraction. Each tissue was also homogenized in 3 ml of 0.2*M* $HClO_4$. The homogenate was centrifuged at 2,500 rpm for 5 min. The pellet was washed by resuspension in 3 ml of 0.2*M* $HClO_4$, followed by centrifugation. The pellet and supernatant were the acid-insoluble and the acid-soluble fractions, respectively.

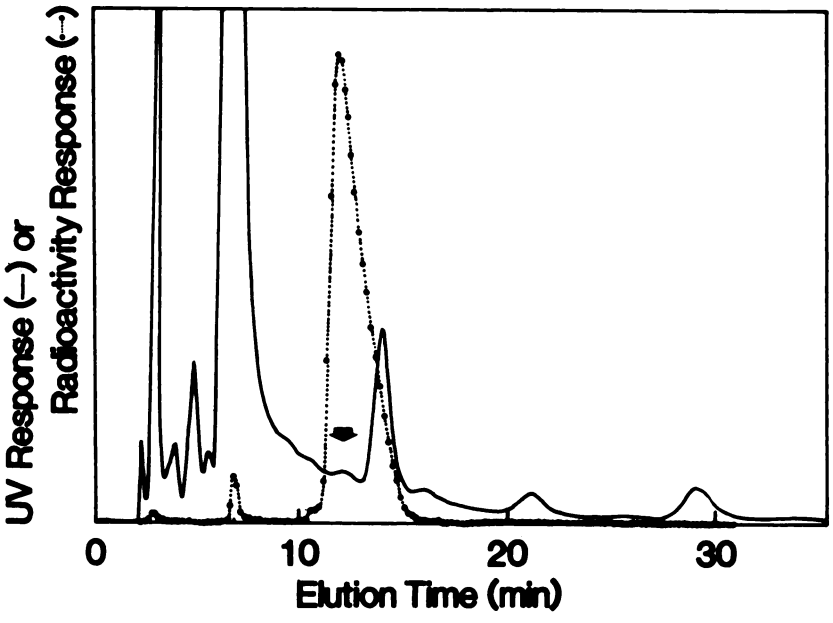

FIGURE 1
Separation of [^{11}C]pargyline on radio-high performance liquid chromatography. Details are described in Materials and Methods. Straight line and dotted line show uv response and ^{11}C radioactivity response, respectively. Arrow shows elution position of authentic pargyline

TABLE 2
Distribution of ^{11}C in Mice After Injection of [^{11}C]Pargyline

Tissue	Uptake (DAR) 1 min (n = 2)*	5 min (n = 3)	10 min (n = 6)	30 min (n = 6)	60 min (n = 4)
Blood	1.00 ± 0.04	0.57 ± 0.19	0.46 ± 0.12	0.24 ± 0.05	0.21 ± 0.01
Heart	1.06 ± 0.10	0.78 ± 0.06	0.84 ± 0.28	0.52 ± 0.16	0.50 ± 0.12
Lung	4.13 ± 0.89	2.00 ± 0.35	1.33 ± 0.46	0.97 ± 0.34	0.98 ± 0.22
Liver	1.26 ± 0.30	1.21 ± 0.23	1.56 ± 0.43	1.03 ± 0.39	0.95 ± 0.26
Pancreas	0.63 ± 0.01	0.91 ± 0.26	1.64 ± 0.52	1.49 ± 0.72	1.58 ± 0.52
Spleen	0.32 ± 0.04	0.78 ± 0.03	1.15 ± 0.29	0.88 ± 0.36	1.26 ± 0.12
Small intestine	0.98 ± 0.09	0.83 ± 0.17	1.38 ± 0.50	1.17 ± 0.50	1.26 ± 0.52
Kidney	3.39 ± 0.55	2.66 ± 0.32	3.19 ± 1.51	2.83 ± 1.82	1.85 ± 0.54
Muscle	0.43 ± 0.07	0.37 ± 0.06	0.67 ± 0.16	0.43 ± 0.16	0.30 ± 0.06
Brain	1.01 ± 0.16	0.46 ± 0.06	0.53 ± 0.21	0.34 ± 0.14	0.31 ± 0.10
Testis	0.23 ± 0.02	0.28 ± 0.01	0.59 ± 0.40	0.35 ± 0.17	0.31 ± 0.10
Bone	0.41 ± 0.35	0.35 ± 0.06	0.59 ± 0.21	0.44 ± 0.14	0.35 ± 0.12

* n = No. of mice. Errors are 1 s.d.

Autoradiogram in the mouse brain

A mouse was injected i.v. with [^{11}C]pargyline (2.0 mCi). After 20 min, the brain was removed, frozen on dry ice, and cut into 30-μm-thick slices using an autocryotome (LKB). The slices were dried at 40°C on a hot-plate, and XAR-5 film¶ was exposed for 3 hr and then developed.

Positron emission tomography in the rabbit heart and lung

A male rabbit was injected i.v. with [^{11}C]pargyline (2.0 mCi). An emission scan of the heart and lung region from the time of injection to 30 min and of the brain region from 46 min to 60 min was performed using an ECAT-II scanner** with medium resolution mode. The blood was collected at the indicated time intervals. The blood concentration is expressed as the DAR. The uptakes in the heart and lung were also expressed as a differential absorption ratio (DAR-ECAT), (count/pixel) × (g body weight/total injected count).

RESULTS

Synthesis of [^{11}C]pargyline

Carbon-11 pargyline was synthesized with a radiochemical yield of 22–45% and with a radiochemical purity of over 99% in 50–60 min. Figure 1 shows the radio-HPLC chromatogram for a preparation of [^{11}C]pargyline. Table 1 summarizes the results of seven experiments. Below a reaction temperature of 60°C, most of the methylated product was [^{11}C]pargyline. The HPLC retention time (12 min) was identical to that of authentic pargyline. At 65°C several radioactive impurities with retention times of 3–7 min and 20 min were observed. In many cases, [^{11}C]pargyline was obtained with a radiochemical purity of over 99%, but a part of [^{11}C]pargyline was degraded when the [^{11}C]pargyline fraction obtained by the preparative HPLC was evaporated in the more acidic solvent.

Biodistribution in mice

Table 2 shows the biodistribution of the [^{11}C]pargyline in mice. The [^{11}C]pargyline was transported well into the many organs and was cleared rapidly from the blood. In the kidney, the highest uptake and slowest clearance were observed. The liver uptake pattern was similar to that of the kidney. In the lung, the highest uptake occurred just after injection, the clearance was rapid for the first 10 min and very slow thereafter. In the brain and heart, the ^{11}C was cleared slowly. In the pancreas, spleen and small intestine, it was accumulated for the first 10 min and maintained. Generally, equilibrium levels of the ^{11}C were reached after 30 min.

Table 3 shows the effect of the loading doses on the distribution of the [^{11}C]pargyline. In the several organs, the uptakes (DAR) tended to be lower with the higher doses, but the difference was small. However, the mass of pargyline in each organ increased with loading dose.

Autoradiogram in the mouse brain

Figure 2 shows the autoradiograms of [^{11}C]pargyline in the mouse brain. The amygdala and cerebral venticles showed higher uptakes than other regions.

Subcellular distribution

The subcellular distributions were examined in the brain, lung, liver, and kidney (Table 4). High proportions of ^{11}C radioactivity were observed in the nuclear and crude mitochondrial fractions. The proportions of the ^{11}C in the two fractions in the brain were larger than those in other organs. In the brain and liver, the proportions of the ^{11}C in the crude mitochondrial fractions

TABLE 3
Effect of Loading Dose on Distribution of [^{11}C]Pargyline in Mice at 30 min After Injection*

Tissue	Loading dose: 30–60 μg/kg† (n = 6)	0.5 mg/kg (n = 4)	5 mg/kg (n = 4 Uptake (DAR)	50 mg/kg (n = 4)	50 mg/kg (n = 4) (before 2 hr)*
Blood	0.24 ± 0.05	0.24 ± 0.03	0.23 ± 0.04	0.32 ± 0.02	0.24 ± 0.03
Heart	0.52 ± 0.16	0.48 ± 0.02	0.37 ± 0.04	0.44 ± 0.04	0.40 ± 0.04
Lung	0.98 ± 0.34	0.96 ± 0.09	0.74 ± 0.05	0.80 ± 0.08	0.75 ± 0.08
Liver	1.03 ± 0.39	1.40 ± 0.10	1.31 ± 0.20	1.25 ± 0.05	1.06 ± 0.14
Pancreas	1.49 ± 0.72	2.27 ± 0.44	2.00 ± 0.51	1.40 ± 0.27	1.27 ± 0.23
Spleen	0.88 ± 0.36	1.05 ± 0.08	0.98 ± 0.08	0.94 ± 0.10	0.79 ± 0.04
Small intestine	1.17 ± 0.50	1.39 ± 0.29	1.14 ± 0.04	1.03 ± 0.17	1.07 ± 0.18
Kidney	2.83 ± 1.83	2.94 ± 0.64	2.00 ± 0.28	2.02 ± 0.60	2.28 ± 0.94
Muscle	0.43 ± 0.16	0.40 ± 0.12	0.37 ± 0.05	0.55 ± 0.19	0.59 ± 0.20
Brain	0.34 ± 0.14	0.32 ± 0.04	0.22 ± 0.03	0.34 ± 0.06	0.27 ± 0.02

* Carrier pargyline (50 mg/kg) was administered at 2 hr before injection of [^{11}C]pargyline.
† No carrier added.

were larger than those in the nuclear fractions, but the reverse was observed in the lung and kidney. The ^{11}C in the acid-insoluble fraction increased with time, and its proportion reached 60–70% of the total radioactivity at 60 min. When carrier pargyline (63 mg/kg) was injected simultaneously, the proportions of ^{11}C in the nuclear and crude mitochondrial fractions were lower than in the no carrier added experiment.

Positron emission tomography in a rabbit

Figure 3 (left) shows the positron emission tomogram of the [^{11}C]pargyline in the heart and lung region of a rabbit. Figure 3 (right) shows the blood clearance and the heart and lung uptakes measured by the quantitative data collected in a time sequential study. Uptakes of the [^{11}C]pargyline in the heart were constant for 30 min. But in the lung, it decreased gradually for the first 20 min and then remained constant; the blood clearance was rapid for the first 10 min.

DISCUSSION

Many propynylamines irreversibly inhibit MAO by forming covalent adducts between the flavine of MAO and their propynyl groups (*3–6*). Among these inhibitors, pargyline has been more extensively investigated

TABLE 4
Subcellular Distribution of [^{11}C]Pargyline in Mouse Tissues (n = 2)

Tissue	Fraction	10 min (%)	30 min (%)	30 min (+63 mg/kg) (%)	60 min (%)
Brain	Nuclear Fr.	11.3	23.2	13.3	14.3
	Crude mitochondrial Fr.	34.2	37.9	23.7	32.5
	Post mitochondrial Fr.	56.3	38.9	63.0	53.3
	Acid-insoluble Fr.	38.2	46.1	—	58.6
Lung	Nuclear Fr.	16.5	28.2	16.6	25.3
	Crude mitochondrial Fr.	9.3	13.3	7.8	12.1
	Post mitochondrial Fr.	74.2	58.5	80.6	62.6
	Acid-insoluble Fr.	41.3	56.8	—	58.6
Liver	Nuclear Fr.	5.0	13.7	17.1	7.5
	Crude mitochondrial Fr.	15.4	21.3	11.2	19.1
	Post mitochondrial Fr.	79.6	65.1	71.7	73.4
	Acid-insoluble Fr.	38.7	46.8	—	67.5
Kidney	Nuclear Fr.	14.5	15.1	10.6	32.9
	Crude mitochondrial Fr.	7.0	9.6	6.7	8.9
	Post mitochondrial Fr.	78.5	75.3	82.7	58.2
	Acid-insoluble Fr.	36.1	37.8	—	69.8

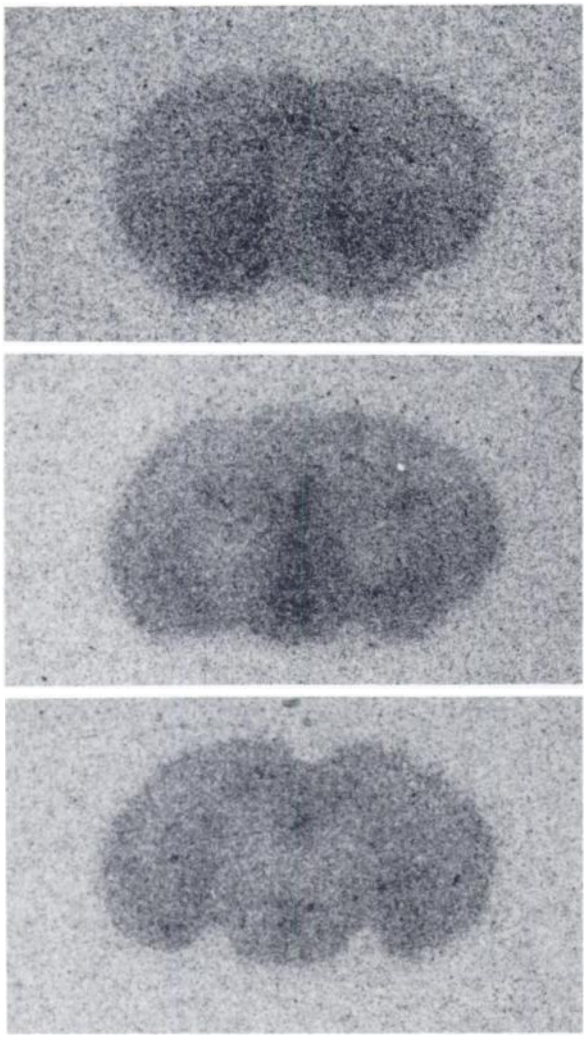

FIGURE 2
Autoradiogram of [^{11}C]pargyline in mouse brain

and has a high degree of specificity for the Type B MAO. The [^{11}C]pargyline was accumulated in many organs and its concentrations were constant after 30 min (Table 2, Figure 3 (left)). Relative uptakes in the mouse heart and lung were different from those in a rabbit. In the mouse brain, lung, liver, and kidney, high proportions of ^{11}C radioactivity were incorporated into the acid-insoluble materials with time, and most was present in the crude mitochondrial and nuclear fractions (Table 4), which suggests that high proportions of [^{11}C]pargyline bind to MAO. The concentrations of MAO were shown to be different in organs of the same species and in different animal species. MAO is tightly bound to the mitochondrial outer membrane and makes an irreversible complex with pargyline (*3–5*). Erwin and Deitrich have shown that the subcellular distribution of [^{14}C]pargyline binding is similar to that of MAO in the rat liver in vivo (*12*). Therefore, the levels of ^{11}C in the organs may reflect the concentration of MAO. Correlation between the relative uptakes of the [^{11}C]pargyline and the relative in vitro MAO activities between six organs (*13,14*) is shown in Table 5. In a mouse, the uptakes of the [^{11}C]pargyline in the liver and lung were higher than in the brain (as is the Type B MAO activities), but in spite of no Type B MAO activity in the kidney and spleen, a high uptake of the [^{11}C]pargyline was observed. In addition, the higher pargyline doses did not influence the distribution (Table 3), although the proportions of the ^{11}C in the nuclear and crude mitochondrial fractions were less in the highest loading dose (Table 4). The quantity of pargyline in the mouse livers at 30 min after injection of the highest loading dose (50 mg/kg) was calculated to be 320 nmol/g liver. This value is probably far in excess of the number of MAOs. In the rat livers, the number of MAOs has been estimated. Egashira et al. (*15*) have calculated the quantity of Type B MAOs per mitochondrion to be 20,000 molecules assuming the number of mitochondria per g of rat liver to be 11×10^{10} (*16*). This value is equivalent to 47 nmol/g mitochondrial protein or 3.7 nmol/g liver (*15*). Parkinson and Callingham have indicated in the in vitro experiment

TABLE 5
Relative Uptakes of [^{11}C]Pargyline and Relative MAO Activities*

	Mouse				Rabbit			
	Uptake (min)		MAO†		Uptake (min)		MAO‡	
	30	60	Type A + B	Type B	25–30	46–60	Type A	Type B
Brain	100	100	100	100		100	100	100
Heart	153	161			262		26	27
Lung	285	316	153	257	145		67	55
Liver	303	306	142	596			79	196
Spleen	259	406	51	0			57	35
Kidney	832	597	117	0			160	132

* Uptakes of [^{11}C]pargyline and MAO in mouse and rabbit tissues were normalized to those in the brain at 100.

† Enzymatic activities of Type A + B and Type B were measured with the substrates 5-hydroxytryptamine (10 m*M*) and benzylamine, respectively (*9*).

‡ Enzymatic activities of Type A and Type B were measured with the substrates 5-hydroxytryptamine (0.1 m*M*) and phenylethylamine, respectively (*10*).

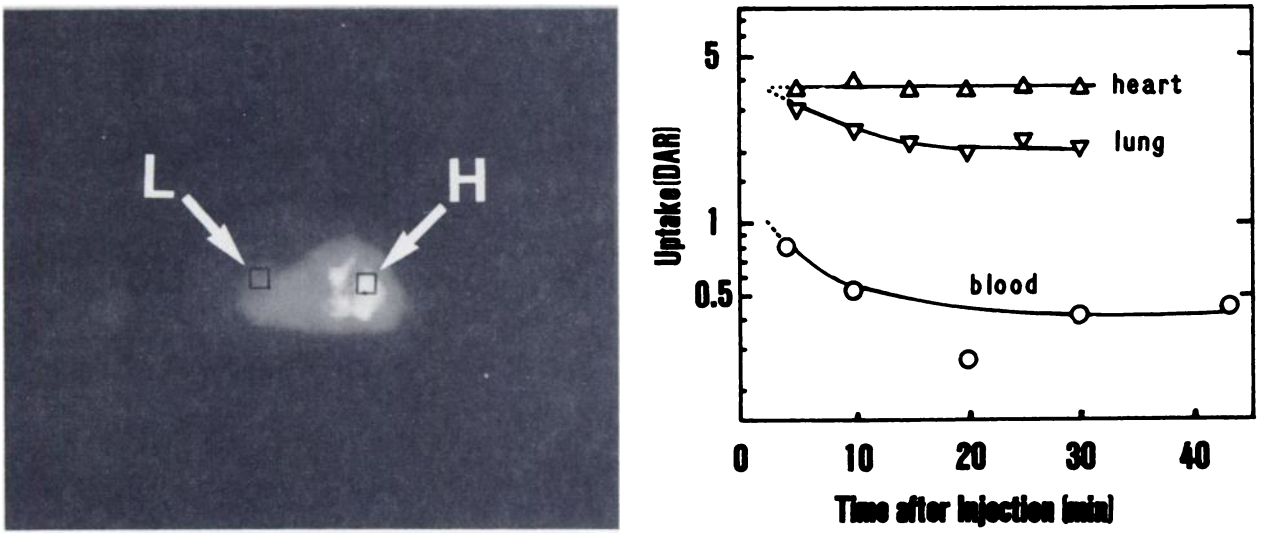

FIGURE 3
Distribution of [^{11}C]pargyline in rabbit. Left: Positron emission image in rabbit heart and lung region at 25–30 min after injection. Right: Changes in ^{11}C concentration in heart (△), lung (▽) and blood (○). Concentration in heart and lung were calculated in areas shown H and L, respectively, in Fig. 3 (left)

that the pargyline is bound in the rat liver mitochondria in a biphasic manner and the nonspecific binding is increased with the higher loading dose, and that the specific binding of pargyline reaches saturation at 31 nmol/g mitochondrial protein (*17*). Erwin and Deitrich (*12*) have showed that most of the [^{14}C]pargyline binds irreversibly to the macromolecule, probably MAO, in the rat liver in vivo at 12 hr after the injection with loading dose of 20 mg/kg, and that subcellular distribution of the pargyline corresponds to that of MAO. They did not consider at all the nonspecific binding of the pargyline.

In the preliminary PET study of the rabbit, the uptakes of [^{11}C]pargyline were higher in the heart and lung than in the brain, although the reverse correlation was reported in Type B MAO activities (Table 5). However, the data were not enough to estimate the uptakes of the [^{11}C]pargyline in the rabbit because of only one trial and low resolution (full width at half maximum is 15 mm) of the positron camera.

In conclusion, our results indicate that for low doses the uptakes of [^{11}C]pargyline reflect the MAO concentration in the brain, heart, and lung, but further studies are required to elucidate whether the regional distribution of [^{11}C]pargyline in the brain (Fig. 2) also reflects the distribution of MAO. However, for the higher loading doses the trapping of [^{11}C]pargyline in the organs is partly dependent on the nonspecific binding as the results in the in vitro experiments indicate (*17*) in spite of pargyline's high specificity for MAO.

In correctly evaluating the concentration of enzymes in vivo experiments by using suicide inactivators, we should select compounds which are more specific for the enzyme or we need some way of distinguishing between specific and nonspecific uptake.

FOOTNOTES

* Aldrich.

† 8 mm IDX 10 cm, Waters, Radial Compression Separation System.

‡ Sigma Chemical Corporation.

§ Packard Instrument Co., Inc. Downers Grove, IL AUTO-GAMMA 500.

¶ Eastman Kodak Company, Rochester, NY

** Computer Technology & Imaging, Knoxville, TN (formerly: EG&G Ortec)

ACKNOWLEDGMENTS

This work was supported by a Grant-in-Aid for Scientific Research No. 58870064, Ministry of Education, Science and Culture, Japan. The authors are grateful to Dr. K. Itoh for useful advice and discussion on the positron emission tomographic study. The preparation of the typescript by Miss M. Saito and the operation of the cyclotron by the members of Cyclotron and Radioisotope Center are also acknowledged.

REFERENCES

1. Phelps ME, Mazziotta JC, Huang S-C: Study of cerebral function with positron computed tomography. *J Cereb Blood Flow Metab* 2:113-162, 1982
2. Rando RR: Chemistry and enzymology of k_{cat} inhibitors. *Science* 185:320-324, 1974
3. Houslay MD, Tipton KF, Youdim MBH: Multiple forms of monoamine oxidase: Fact and artefact. *Life Sci* 19: 467-478, 1976
4. Oreland L, Kinemuchi H, Yoo BY: The mechanism of

action of the monoamine oxidase inhibitor pargyline. *Life Sci* 13:1533–1541, 1973
5. Chuang HYK, Patek DR, Hellerman L: Mitochondrial monoamine oxidase. Inactivation by pargyline. Adduct formation. *J Biol Chem* 249:2381–2384, 1974
6. Maycock AL, Abeles RH, Salach JI, et al: The structure of the covalent adduct formed by the interaction of 3-dimethylamino-1-propyne and the flavine of mitochondrial amino oxidase. *Biochemistry* 15:114–125, 1976
7. Fowler JS: The synthesis of ^{14}C-labeled suicide inactivators of monoamine oxidase. *J Label Compd Radiopharm* 14:435–437, 1978
8. Williams CH: Synthesis of ^{14}C-labelled inhibitors of monoamine oxidase. *J Label Compd Radiopharm* 18: 1545–1548, 1981
9. Iwata R, Ido T, Saji H, et al: A remote-controlled synthesis of ^{11}C-iodomethane for the practical preparation of ^{11}C-labeled radiopharmaceuticals. *Int J Appl Radiat Isotopes* 30:194–196, 1979
10. Iwata R, Ido T: Automated synthesis of $^{11}CH_3I$. *CYRIC Annual Report:* 135–139, 1981
11. Ujiie A, Koyama K, Ido T, et al: Synthesis of C-11 tamoxifen and its biodistribution. *CYRIC Annual Report:* 103–107, 1983
12. Erwin VG, Deitrich RA: The labeling in vivo of monoamine oxidase by ^{14}C-pargyline: A tool for studying the synthesis of the enzyme. *Mol Pharmacol* 7:219–228, 1971
13. Hope DB, Smith AD: Distribution and activity of monoamine oxidase in mouse tissues. *Biochem J* 74: 101–107, 1960
14. Edwards DJ, Malsbury CW: Characteristics of monoamine oxidase in brain and other organs of the golden hamster. *Biochem Pharmacol* 32:959–963, 1978
15. Egashira T, Ekstedt B, Kinemuchi H, et al: Molecular turnover numbers of different forms of mitochondrial monoamine oxidase in rat. *Med Biol* 54:272–277, 1976
16. Gear ARL, Bednarek JM: Direct counting and sizing of mitochondria in solution. *J Cell Biol* 54:325–345, 1972
17. Parkinson D, Callingham BA: The binding of [^3H]pargyline to rat liver mitochondrial monoamine oxidase. *J Pharm Pharmacol* 32:49–54, 1980